Doxorubicin-Loaded Carboxymethyl Cellulose/Chitosan/ZnO Nanocomposite Hydrogel Beads as an Anticancer Drug Carrier Agent

Aung Than Htwe[1,2], Hninn Wutt Yee Htun[1,3], Yamin Thet[1], May Thazin Kyaw[1], Ngwe Sin[1], Win Pa Pa Phyo[1], Cho Cho*
[1]Department of Chemistry, University of Yangon, Myanmar
[2]Department of Chemistry, Mohnyin University, Myanmar
[3]Department of Chemistry, Sittway University, Myanmar

Abstract

In this study, nanocomposite hydrogel beads were prepared by combining carboxymethyl cellulose (CMC), chitosan (CS), and ZnO nanoparticles (ZnO NPs). The obtained nanocomposite hydrogel beads were used as a potential candidate for controlled release of anticancer drug doxorubicin (DOX). The nanocomposite hydrogel beads were characterized using FT-IR, XRD, UV–vis, SEM, TG-DTA analysis. Then antimicrobial activity of the nanocomposite hydrogel beads was tested for the purpose of using nanocomposite hydrogel beads in biomedical application. In addition, gel content, swelling properties, and drug release of the samples were evaluated. The swelling and drug release profiles revealed that the amount of drug released and swelling of the hydrogels depended on the CMC/CS content, pH, and ZnO nanoparticle content. Prolonged and more controlled drug releases were observed for ZnO nanoparticle containing CMC/CS beads, which increased with the rise in ZnO nanoparticle content.

Keywords: nanocomposite hydrogel beads, carboxymethyl cellulose, chitosan, ZnO nanoparticles, drug release

1. Introduction

Developing effective cancer treatments is crucial because, in recent years, cancer has posed a serious threat to people's health all over the world. Chemotherapy, radiation therapy, and surgery are the standard cancer treatment options (Wang *et al.*, 2020). A three-dimensional (3D) network of polymers with a specific ratio of hydrophilic and hydrophobic components makes up a hydrogel (Azady *et al.*, 2021). Due to their brittle networks after reaching their maximum swelling, hydrogels are not mechanically robust enough, which limits their usage (Gaharwar *et al.*, 2014; Satarkar *et al.*, 2010). In addition to their biocompatibility, ability to simulate the extracellular matrix, ability to encapsulate and distribute cells and medicines, and ability to mimic the extracellular matrix, hydrogels are employed in a variety of biomedical applications (Catton *et al.*, 2021). Wang *et al*. (2020) found that three-dimensional polymeric hydrogel networks can sustainably release drugs by swelling and contracting while holding water. In order to meet the demand for materials with improved and predictable mechanical properties and usefulness, nanocomposite hydrogels have been created by adding nanoparticles to a hydrogel matrix (Azady *et al.*, 2021). The synthetic anionic modified cellulose, which is known as carboxymethyl cellulose (CMC), is formed by carboxymethylation of cellulose. CMC possesses eco-friendly properties such as safety, biodegradability, biocompatibility, non-toxicity, and

*Cho Cho, Department of Chemistry, University of Yangon

sensitivity to different environments (Wang *et al.*, 2020; Cai *et al.*, 2021). The presence of the anionic carboxylate group COO allows the polyelectrolytic CMC chains to interact with other oppositely charged polyelectrolytes (e.g., chitosan) to form a 3-dimensional polyelectrolyte complex hydrogel network. Covalent cross-linking can be achieved in the presence of citric acid or glutaraldehyde to form hemiacetal (Lotfy *et al.*, 2020). Chitosan is a natural cationic polymer produced by the deacetylation of chitin extracted from shrimp peel. Chitosan is a natural polysaccharide containing an amino group and can dissolve in a diluted solution of acetic acid as a result of the protonation of the amino group, forming an NH_3^+ cationic group (Abdelghany *et al.*, 2019; Iqbal *et al.*, 2021). The protonated amino groups allow the formation of chitosan beads by ionic gelation through the interaction with negatively charged ionic salts, such as sodium tripolyphosphate (TPP) (Affes *et al.*, 2021; Nagpal *et al.*, 2010).

Addition of inorganic zinc oxide nanoparticles (ZnO NPs) to polymers is promising since it has a brilliant activity in different applications (Metwally *et al.*,2022). The entrapment of ZnO NPs into polymers leads to a change in the polymeric geometrical structure, which can be used for drug delivery applications (Yadollahi *et al.*, 2016; Singh *et al.*, 2020; Sadhukhan *et al.*, 2019). Moreover, for modulating the drug release profiles, zinc oxide (ZnO) nanoparticles have been incorporated into the hydrogel matrix because of its prominent physical and chemical properties, powerful antibacterial properties, remarkable mechanical strength, good stability, and a low production costs (Li *et al.*, 2010).

The aim of this study was to prepare a series of improved drug release system using polymers, CMC/CS with weight ratios of 1:1, 1:3 and 3:1 containing ZnO NPs, which would allow adjusting controlling the final release characteristics of the formulation. The prepared nanocomposite beads were characterized using the modern techniques including XRD, FTIR, SEM, TG-DTA, and UV-vis. Then, the antimicrobial activity of the prepared nanocomposite beads were studied. The effect of the concentration of the ZnO NPs was examined on gel content, swelling ratio, and drug loading and release behavior test. Doxorubicin was loaded into the nanocomposite beads as a model drug with the release of the drug from the nanocomposite hydrogels investigated.

2. Materials and Methods

2.1. Materials

Asparagus stalk end was purchased from Htauk Kyant Market, Mingalardon Township, Yangon, Myanmar. All chemicals used in this study were manufactured by British Drug House Chemicals Ltd. (BDH).

2.2. Preparation of Carboxymethyl Cellulose from Asparagus Stalk End Powder

Firstly, cellulose was prepared from asparagus stalk end powder according to the method of Klunklin *et al.*, 2021; Rodsamran *et al.*, 2017; and Rachtanapun *et al.*, 2011. Secondly, to prepare carboxymethyl cellulose (CMC), obtained cellulose was treated with 30% NaOH,

isopropanol and mono chloroacetic acid by chemical method (Aung Than Htwe *et al.*, 2022). Obtained CMC was dried in oven at 55 ºC for 12 h. The final CMC product was in powder form.

2.3. Preparation of Zinc Oxide Nanoparticles

100 mL of 0.1 M zinc sulphate heptahydrate ($ZnSO_4.7H_2O$) solution was heated at 60 °C under stirring at 750 rpm and then 15 mL of 3 % chitosan solution was added drop-by-drop to constant stirring. The resultant solution was adjust to pH 12 by adding of 1 M NaOH solution which resulted in white cloudy cream-colored zinc hydroxide precipitate formation. For the complete reduction in zinc hydroxide, the reaction mixture was left for 2 h in same condition. Then the precipitate was centrifuged at 5,000 rpm for 20 min at room temperature by distilled water followed by ethanol repeatedly in order to remove the impurities. The precipitate was dried overnight in an oven at 100 °C. The obtained dried powder was calcined in a muffle furnace at 600 °C for 2 h and the white powder of ZnO NPs was obtained after calcination.

2.4. Preparation of Carboxymethyl Cellulose/Chitosan Nanocomposite Hydrogel Beads Containing ZnO Nanoparticles

The 3 g of chitosan(CS) flake was dissolved in 3 % v/v acetic acid solution to obtain 3% v/v CS solution by using magnetic stirrer at room temperature for 2 h. 3 g of CMC powder was dissolved in 100 mL distilled water at 75 °C for 6 h to obtain a viscous solution. After cooling, the CMC solution and CS solution with volume ratios of 3:1, 1:1, and 1:3 were mixed through stirring for 2 h until a homogeneous solution. Then, different amounts of ZnO nanoparticles (0%, 5%, 10%, and 15%) were dispersed in 10 mL of distilled water in each. Then, it was added slowly into the CMC/CS solution and stirred for 6 h to obtain viscous solution. After that, viscous solution containing CMC/CS and ZnO nanoparticles was transferred using a syringe in the form of droplets into 400 mL of 1M sodium hydroxide solution. The beads stayed in NaOH solution for 48 h. And then, they were washed with distilled water to remove unreacted NaOH on the surface of the beads and dried at 50 °C under vacuum oven for 6 h. The weight ratios of the components of CMC/CS/ZnO (CCZ) nanocomposite beads were shown in Table 1.

2.5 Characterization

The functional groups of the CMC, ZnO NPs and all CCZ were determined by using Perkin Elmer GX System FT IR spectrophotometer. Transmission level measured at the wavenumber range of 4000–400 cm^{-1}. The X-ray diffraction (XRD) measurements of the CMC, ZnO NPs and all CCZ were recorded using Shimadzu 8000 X-ray diffractometer (Shimadzu, Japan) with a detector operating under a voltage of 40.0 kV and a current of 30.0 mA using Cu Kα radiation (λ = 0.15418 nm). The recorded range of 2θ was 10–80°, and the scanning speed was 6°/min. The surface morphology of CMC, ZnO and CCZ materials was studied using SEM (EVO-18, Probe Micro Analyzer, Germany). SEM images of samples were collected under an accelerating voltage of 5 kV. The thermal stability of CMC, ZnO NPs and all CCZ was evaluated by a simultaneous TG-DTA (DTG- 60H) operated under a nitrogen atmosphere. The samples of

about 8 mg each were weighed into solid aluminum pans without seals. The measurement was carried out at a heating rate of 20.0 °C per minute and scanned from 40 °C to 600 °C.

Table 1. Volume ratio of components in CMC/CS/nZnO nanocomposite hydrogel bead

Components number	Volume ratio		ZnO NPs (%)
	3 % CS solution	3 % CMC solution	
CCZ1	1	1	0
CCZ2	1	3	0
CCZ3	3	1	0
CCZ4	1	1	5
CCZ5	1	3	5
CCZ6	3	1	5
CCZ7	1	1	10
CCZ8	1	3	10
CCZ9	3	1	10
CCZ10	1	1	15
CCZ11	1	3	15
CCZ12	3	1	15

2.6 Determination of Gel content

About 0.1 g of CCZ nanocomposite hydrogel beads was poured in phosphate buffer solution at room temperatur for 2 days. Every 12 h, the phosphate buffer solution was replaced in the sample container to remove soluble parts from the hydrogel after which swollen samples were taken out, dried in an oven at 50 °C, and weighed (Gholamali and Yadollahi, 2020). The gel content of nanocomposites was calculated by the following equation.

$$\text{Gel content (\%)} = \frac{\text{Final weight of dried sample (g)}}{\text{Initial weight of dried sample (g)}} \times 100\ \%$$

2.7 Determination of Swelling Ratio

The swelling ratios of CCZ nanocomposite hydrogel beads were measured in phosphate buffer solutions of pH 1.2, 6.8, and 7.4 at ambient temperature. Specifically, 0.1 g of the prepared hydrogel beads was submerged in 50 mL of phosphate buffer solution (1.2, 6.8, and 7.4) at ambient temperature for 360 min to reach the swelling equilibrium. To measure the swelling ratio, the hydrogels were extracted from the phosphate buffer solution and weighed (Gholamali and Yadollahi, 2020). The swelling ratio of beads was calculated by the following equation.

$$\text{Swelling ratio (\%)} = \frac{\text{Final weight (g)}}{\text{Initial weight (g)}} \times 100\ \%$$

2.8 Determination of Antimicrobial Activity

The antimicrobial activity of CCZ nanocomposite hydrogel beads were carried out by agar disc diffusion method at Pathein University, Myanmar. Eight microorganisms namely

Escheerichia coli, Candida albicans, Bacillus subtilis, Staphylococcus aureus, Pseudomonas fluorescens, Agrobacteriumb tumefaciens, Bacillus pumilis, and *Micrococcus luteus* were used for this test.

2.9 Determination of Drug Loading Study

The loading of doxorubicin(DOX) in CMC, CS and CCZ nanocomposite hydrogel beads was carried out as follows: 0.3 g of the prepared dry hydrogel beads was swollen in 30 mL of aqueous solution containing doxorubicin (200 ppm in distilled water). After continuous stirring at 25 °C for 48 h under dark conditions, the beads were washed. Then, the loading capacity of doxorubicin was determined through measuring its absorbance by UV–vis spectroscopy at 483 nm using the following equation (Gholamali and Yadollahi, 2020).

$$\text{Drug loading (g/g)} = \frac{\text{Weight of the drug in hydrogel (g)}}{\text{Weight of hydrogel (g)}}$$

2.10 Determination of Drug Release Study

0.1 g of CMC, CS and CCZ nanocomposite hydrogel beads containing DOX was immersed under continuous stirring (50 rpm) in 10 mL of the selected release media (pHs 1.2, 6.8, and 7.4) at 37 °C for 24 h. At the assigned time intervals, 5 mL of the release media was collected and the amount of drug released was determined by measuring its absorbance at 483 nm using a UV spectrophotometer. To adjust the total volume of the solution, the volume of the solution was kept constant at the same volume each time after sampling by adding fresh phosphate buffer solution. UV–vis spectroscopy was applied to determine the amount of drug released from the CMC, CS and CCZ nanocomposite hydrogel beads, with the amount of doxorubicin measured using a standard calibration curve obtained under the same conditions.

3. Results and Discussion

3.1 Preparation and Characterization of Carboxymethyl Cellulose/Chitosan Nanocomposite Hydrogel Beads Containing ZnO Nanoparticles

The simple co-precipitation method was used to prepare carboxymethyl cellulose/chitosan/ZnO (CCZ) nanocomposite beads. CMC and chitosan are among the most important biopolymers that can be easily cross-linked via ionic interactions. Figure 1 displays the generation of CMC/CS/ZnO nanocomposite hydrogel beads (Gholamali and Yadollahi, 2020).

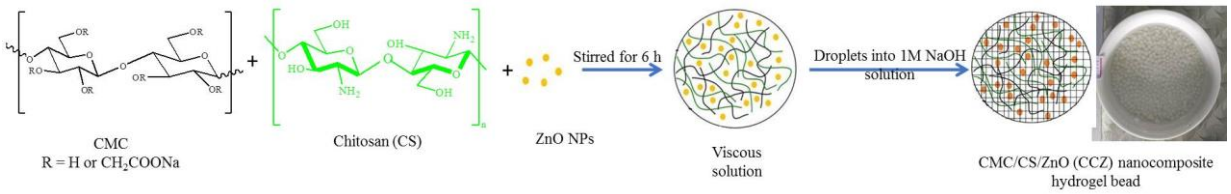

Figure 1. Schematic representation of formation of ZnO NPs in the CMC/CS nanocomposite hydrogel beads

3.2 FT IR Spectra Analysis

The FT IR analyses of CS, CMC, ZnO NPs, and CCZ nanocomposites were carried out, and the data were presented in Figure 2. In the raw CS spectrum (Figure 2(a)), the bands at 3357 and 3293 cm^{-1} were ascribed to stretching vibrations of O–H and N–H in CS. In addition, C–H stretching was shown for common groups, with narrow peaks at 2925 and 2874 cm^{-1}. The absorption bands at 1645 cm^{-1}, between 1375 and 1420 cm^{-1}, and at 1000–1200 cm^{-1} were related to carbonyl stretching of the secondary amide and to C–N and C–O stretching on the polysaccharide skeleton, respectively (Yadollahi *et al.*, 2014). In the CMC spectrum (Figure 2(b)), a broad asymmetrical band was observed at 1645 cm^{-1} and a narrower symmetrical band at 1413 cm^{-1}, which belonged to the basic characteristic functional groups –COO− (Barkhordari *et al.*, 2014). Also, the peak at 1080 cm^{-1} was associated to the stretching of C-O on the polysaccharide skeleton (Gholamali *et al.*, 2019). Figure 2(c) showed that the absorption peaks at the 598 and 440 cm^{-1} assigned to Zn-O stretching thus confirming the existence of ZnO-NPs in the polymer network.

Figure 2(d), (e) and (f) showed that the FTIR spectra of all CCZ bio-nanocomposite beads compared with those of the above three samples. It was found that the original hydroxyl signal peaks observed in the FTIR spectra of CMC and CS at 3459 and 3287 cm^{-1} became broader and moved to a lower frequency of 3278 cm^{-1} in the CCZ bead spectrum, suggesting hydrogen bond formation between the carboxyl groups of CMC and hydroxyl groups of CS or superposition of stretching vibrations of $–NH_2$ and –OH groups. Again, sharpening of some small bands at approximately 1400–1600 cm^{-1} and a new absorption band at 1583 cm^{-1} were observed, which could be explained by interactions between the positive amine groups in CS and the negative carboxyl groups in CMC, as well as to some new hydrogen bond formation between CS and ZnO NPs (Sun *et al.*, 2019). Moreover, compared with the spectrum of ZnO NPs, the broad absorption peak observed at about 400-590 cm^{-1} was assigned to Zn-O vibrations, which confirmed the presence of ZnO NPs in the polymer matrix (Upadhyaya *et al.*, 2014; Zare *et al.*, 2019; Gholamali *et al.*, 2019).

3.3 XRD of ZnO NPs and CCZ Nanocomposites

The XRD patterns of ZnO NPs powder and all CCZ nanocomposite beads are shown in Figure 3. Figure 3(a) showed 5 peaks at 2θ = 31.7º, 34.2º, 36.2º, 47.4º and 56.4° which represented different crystalline forms of ZnO. These peaks correspond to (100), (002), (101), (102) and (110) planes of zinc oxide, respectively. Strong and narrow peaks of ZnO NPs showed that it is crystalline in a hexagonal wurtzite structure (Bhuyan *et al.*, 2015).

All the tested CCZ nanocomposite beads exhibited the characteristic diffraction peak at around 2θ = 20° corresponding to a semi-crystalline polymer of chitosan in a chitosan-CMC composite. No change was observed in the position of both peaks after the incorporation of ZnO NPs. Moreover, the peaks corresponding to ZnO NPs were not seen in nanocomposite beads, suggesting that the crystalline structure of polymer was not affected by the presence of ZnO NPs.

In addition, homogenous dispersing and distributing of ZnO NPs in polymer matrix without aggregation and destroying of crystalline structure of ZnO NPs during the composite bead making process, and formation of some interactions between ZnO ions and hydroxyl groups of chitosan (Rhim *et al.*, 2006).

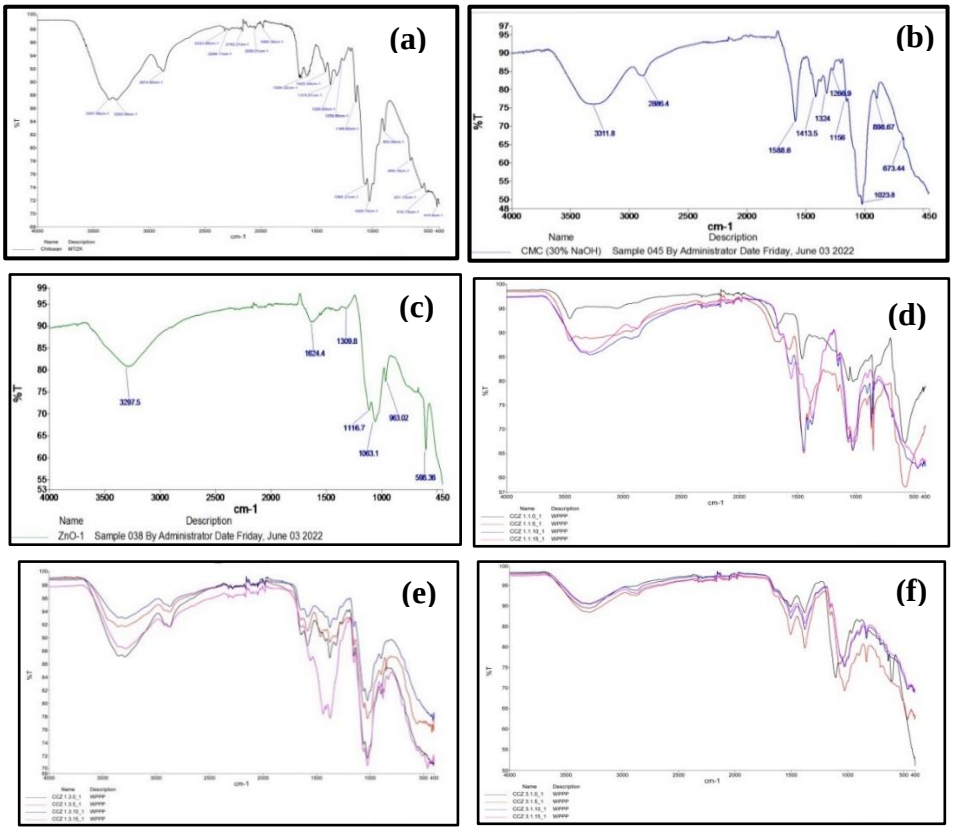

Figure 2. The FTIR spectra of (a) CS, (b) CMC, (c) pure ZnO NPs and (d) 1:1 of CMC/CS bead containing ZnO NPs (e) 1:3 of CMC/CS bead containing ZnO NPs (f) 3:1 of CMC/CS bead containing ZnO NPs

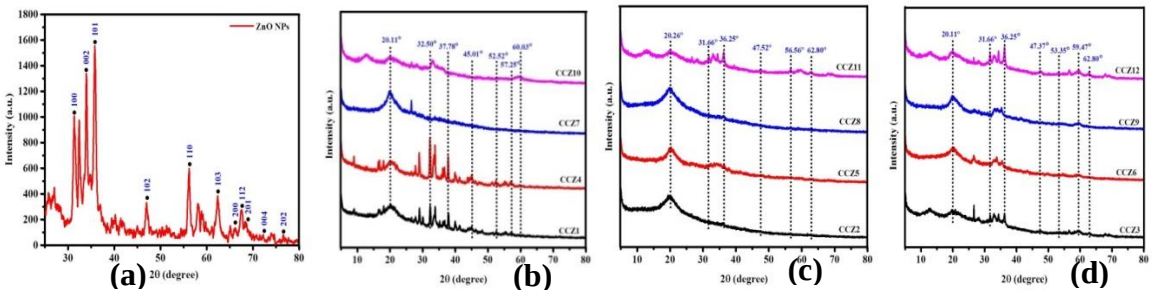

Figure 3. The XRD pattern of (a) pure ZnO NPs and (b) 1:1 of CMC/CS bead containing ZnO NPs (c) 1:3 of CMC/CS bead containing ZnO NPs (d) 3:1 of CMC/CS bead containing ZnO NPs

3.4 SEM of ZnO NPs and CCZ Nanocomposites

SEM images of the native CMC, CS, ZnO/CMC, and ZnO/CMC/CS beads were shown in Figure 4A (a-n) respectively. In addition, after forming the composite with ZnO, the surface of the CMC was altered; the ZnO/CMC showed a crusty surface with several wrinkles (Zare-Akbari *et al.*, 2019). The CCZ bio-nanocomposite beads' surface was less wrinkly and scarcely

had any spaces in the interior zones. Furthermore, some aggregations were found in the matrix of the polymer with an increase in ZnO NP loading in CMC/CS. According to Youssef *et al*. (2016) and Noshirvani *et al*. (2017), ZnO NPs can seem to aggregate in the polymer matrix at increasing concentrations.

Size distributions (Figure 4B a-m) were evaluated by measuring at least 300 particles from SEM micrographs. The results showed that the average diameters of the obtained pure ZnO NPs and nanocomposites were 1.96 μm for ZnO NPs, 1.09 μm for CCZ1, 1.18 μm for CCZ2, 1.52 μm for CCZ3, 0.90 μm for CCZ4, 1.03 μm for CCZ5, 0.91 μm for CCZ6, 0.97 μm for CCZ7, 1.02 μm for CCZ8, 0.78 μm for CCZ9, 0.58 μm for CCZ10, 1.38 μm for CCZ11 and 0.94 μm for CCZ12, respectively. The resulting nanocomposite have a significant size increase (from 0.58 μm for CCZ10 to 1.52 μm for CCZ3), as can be seen from the size distribution histograms. It indicated that the produced nanocomposite possesses wide distribution than ZnO NPs. Finally, the results suggested that the polymer layer was uniformly deposited on ZnO nanoparticle.

3.5 TGDTA of ZnO NPs and CCZ Nanocomposites

Thermogravimetric curves of ZnO NPs and CMC/CS/ZnO NPs bio-nanocomposite beads were presented in Figure 5. It was found that degradation of these samples occurred at three main stages, 80–200°C, 250–350 °C, and 400–550 °C, respectively, which could be attributed to the elimination of the moisture content as hydrogen bound water to the polysaccharide structure (i.e., CMC and CS) and water bound to ZnO NPs, degradation and decomposition of the CMC and CS polymers (amino groups), followed by the formation of carbonaceous residues. As the most prominent feature, the TGA thermograms showed that the temperatures required for CCZ composite beads to lose their half-weights were 320 °C and 360°C compared with 290 °C and 310 °C for CMC and CS, respectively. However, after the addition of ZnO NPs, a sharp decline in the weight loss at 250–300 °C was observed in the CCZ samples which conversely affects (decreased) the thermal stability of the CMC matrix within this specific temperature range. The weight loss values for CCZ1, CCZ2, CCZ3, CCZ4, CCZ5, CCZ6, CCZ7, CCZ8, CCZ9, CCZ10, CCZ11, and CCZ12 samples were 54.41 %, 55.82 %, 65.99 %, 52.47 %, 53.61 %, 62.30 %, 72.63 %, 55.93 %, 49.62 %, 72.57 %, 73.97, and 63.50 % respectively. These data suggest that in addition to increasing the thermal stability of the samples and the residual content, the thermal degradation in the samples containing ZnO-NPs was greater than in the samples without the nanoparticles (Noshirvani *et al.*, 2017; Sun *et al.*, 2019).

The DTA thermograms for all CCZ components were shown in Figure 5b. The thermogram showed the five exothermic peaks for CCZ at 221 °C, 334 °C, 442 °C, 483 °C and 578 °C respectively. The observed early-stage peaks were related to the water loss, but the peaks at higher temperatures were relevant to the oxidative degradation point. The observed differences can lead to changes in polymer networks (Pooresmaeil *et al*., 2018).

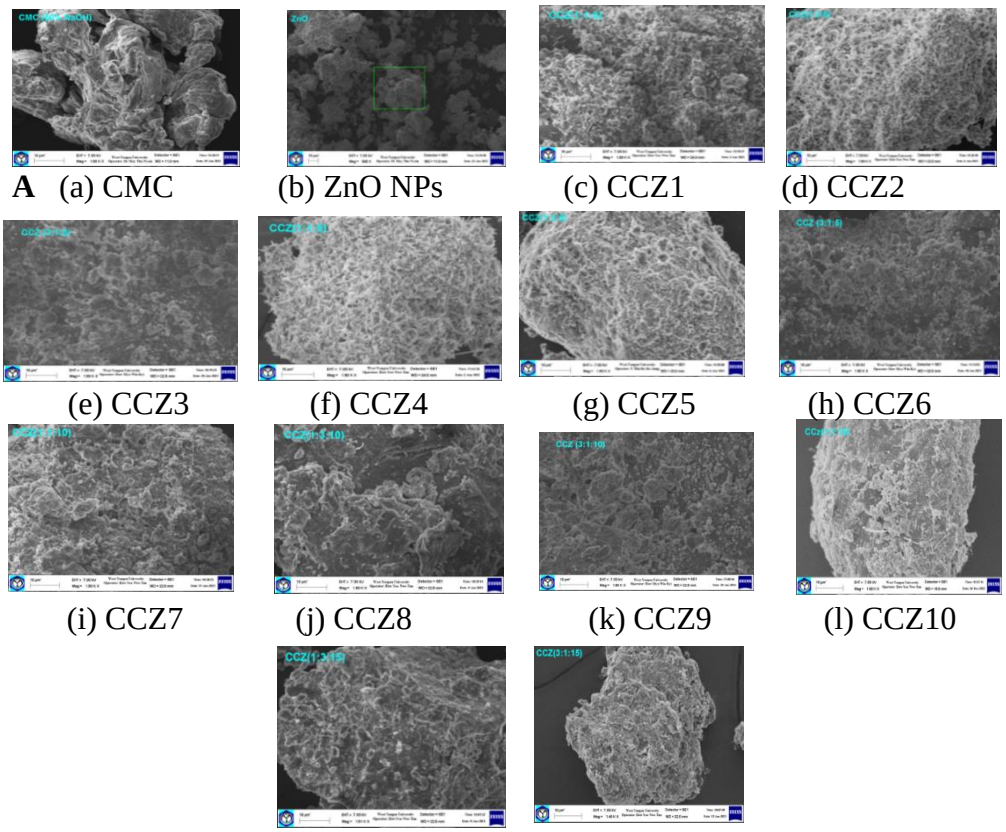

A (a) CMC (b) ZnO NPs (c) CCZ1 (d) CCZ2

(e) CCZ3 (f) CCZ4 (g) CCZ5 (h) CCZ6

(i) CCZ7 (j) CCZ8 (k) CCZ9 (l) CCZ10

(m) CCZ11 (n) CCZ12

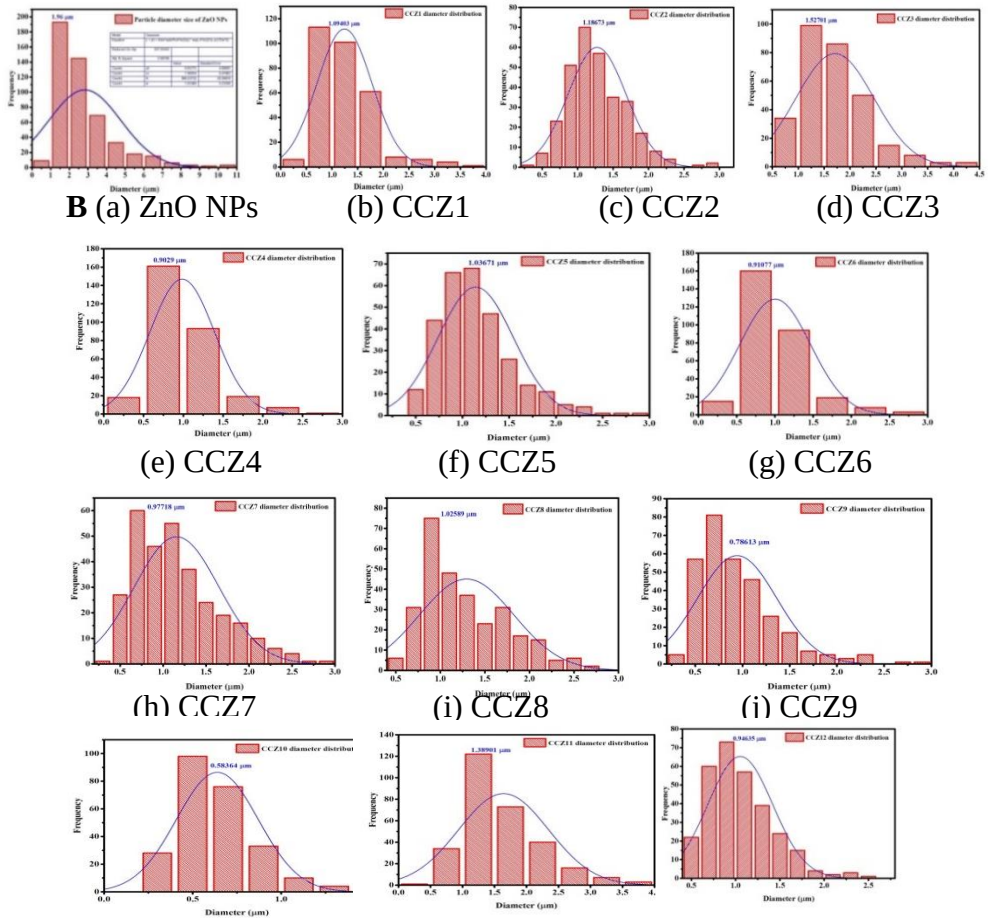

B (a) ZnO NPs (b) CCZ1 (c) CCZ2 (d) CCZ3

(e) CCZ4 (f) CCZ5 (g) CCZ6

(h) CCZ7 (i) CCZ8 (j) CCZ9

(k) CCZ10 (l) CCZ11 (m) CCZ12

Figure 4 (A) SEM images of (a) CMC, (b) ZnO NPs and (c) CCZ 1 to (n) CCZ 12 nanocomposites

(B) Statistical histograms of (a) ZnO NPs and (b) CCZ 1 to (m) CCZ 12

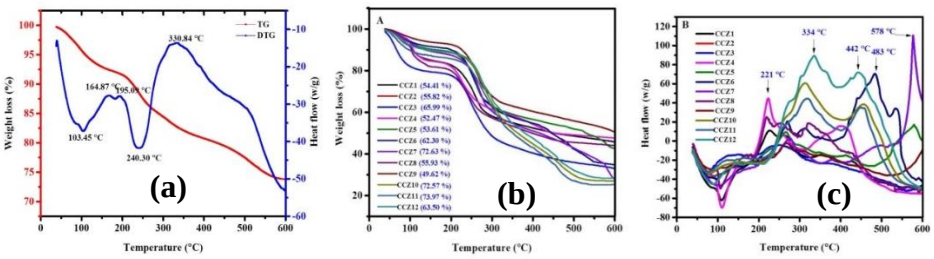

Figure 5. TG-DTA thermograms of (a) ZnO NPs, (b) TGA curves and (c) DTA curves for all prepared CCZ

3.6 UV-Vis of ZnO NPs and CCZ Nanocomposites

The UV–vis spectra of CCZ nanocomposite hydrogel beads were shown in Figure 6. All spectra of the nanocomposite hydrogel beads showed a broad absorption band within the UV range of 200–300 nm because of the surface plasmon resonance effect (Yadollahi *et al.*, 2015). The intensity of the plasmon band grows with increasing the zinc sulphate concentration in the hydrogel beads and reaches higher wave numbers. It can be a result of an increase in the size of ZnO-NPs (Bajpai *et al.*, 2010).

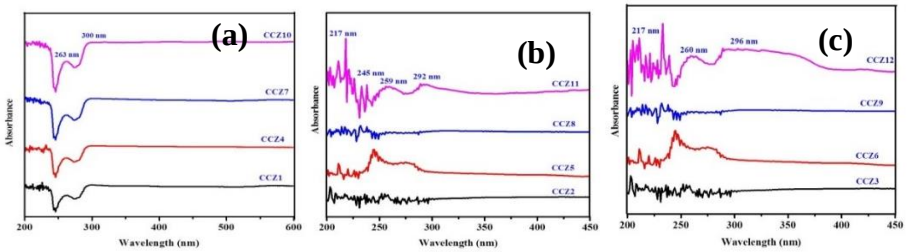

Figure 6. The UV-Vis spectra of (a) 1:1 of CMC/CS bead containing ZnO NPs (b) 1:3 of CMC/CS bead containing ZnO NPs (c) 3:1 of CMC/CS bead containing ZnO NPs

3.7 Antimicrobial of CCZ Nanocomposites

The antimicrobial effect of the CCZ NPs was evaluated by disc diffusion assay against *Bacillus subtilis, Staphylococcus aureus, Pseudomonas fluorescens, Bacillus pumilus, Candida albicans, Escherichia coli, Agrobacterium tumefaciens,* and *Micrococcus luteus*. The results were shown in Figure 7. As the results of the nanoparticles, CCZ NPs had antimicrobial activity. It was found that CCZ1, CCZ4, CCZ5, CCZ6, CCZ8, CCZ9, and CCZ12 NPs do not pronoune the inhibition zone respectively. Whereas CCZ2, CCZ3, CCZ7, CCZ10, CCZ11, and CCZ12 NPs exhibited an inhibition zone diameter against all tested microorganisms. It can be concluded that, according to the antimicrobial activity, the CCZ2 NPs may be intended to use the antibiotic agent.

3.8 Gel content and swelling behavior of CCZ Nanocomposites

The gel content indicated the cross-linking of polymer chains in the hydrogel structure. The crystallinity and the degree of cross-linking depend on the interaction between the components of the hydrogel. Figure 8 showed the gel content between 45 % and 89 % which was variable. The gel content increased with elevation of the CS ratio in the hydrogel structure

and decreased with increasing the CMC ratio. Thus, while the CMC cross-linked, the gel content decreased. Hence, the interaction between CS and other gel components affected the amount of ZnO NPs and it can be used to control the flexibility and strength of the prepared hydrogels. In addition, by increasing the amount of ZnO nanoparticles for 5 % in the hydrogel structure, the gel content would diminish (Niknia *et al.*, 2017; Zarrinkhameh *et al.*, 2015). However, if the amount of ZnO NPs increased to 10 % and 15 %, the gel content increased, wherewith elevation of the amount of ZnO NPs, the interaction between the functional groups of the nanoparticles and the biopolymer chains increased (Gholamali *et al.*, 2019).

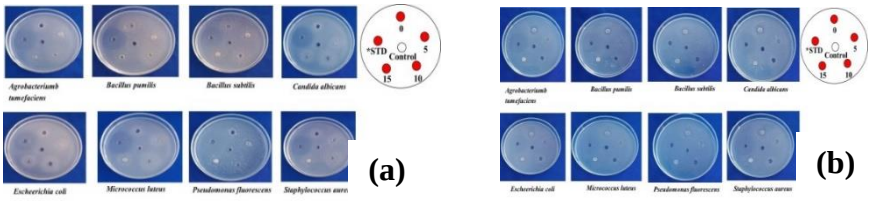

(a) (b)CMC/CS of 1:3 bead containing ZnO NPs

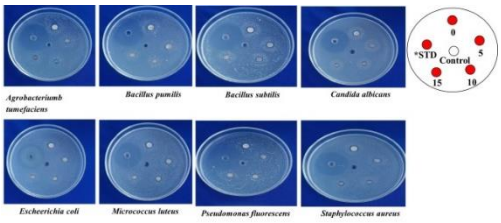

Figure 7. Antimicrobial activities of (a) 1:1 of CMC/CS bead containing ZnO NPs (b) 1:3 of CMC/CS bead containing ZnO NPs (c) 3:1 of CMC/CS bead containing ZnO NPs

Table 2. Inhibition Zone Diameters of CCZ Nanocomposites against Microorganisms by Agar Well Diffusion Method

Tested microorganisms	Inhibition Zone Diameters (mm)					
	CCZ2	CCZ3	CCZ7	CCZ10	CCZ11	*STD
A. tumefacians	14.5	10.6	9.5	9.2	10.3	27.5
B. pumilus	13.0	10.7	9.4	9.2	10.7	26.3
B. subtilus	14.2	10.9	9.6	9.3	10.5	27.2
C. albicans	14.1	10.5	9.5	9.1	10.2	27.6
E. coli	14.0	11.1	9.7	9.2	10.3	27.1
M. leteus	12.7	10.8	9.4	9.3	10.0	26.5
P. fluorescens	13.9	10.5	9.7	9.4	10.1	27.6
S. aureus	14.5	10.9	9.6	9.1	10.4	27.7

For Bacterial *STD = Chloramphenicol
For Fungus *STD = Nystatin

Agar well diameter – 8 mm
10 mm – 14 mm = low activity
15 mm – 19 mm = good activity
20 mm and above = very high activity

3.9 Swelling Behaviour

The swelling behavior of the bionanocomposite hydrogel beads was analyzed in the pH of 1.2, 6.8 and 7.4 in order to study the pH sensitivity of the prepared beads. Figure 9 shows the degree of swelling of bionanocomposite beads enhanced with time, first rapidly and then slowly,

reaching a maximum constant swelling. It was observed that the swelling degree of prepared beads at pH 7.4 and 6.8 was higher than that of pH 1.2, as in the higher pH (6.8 and 7.4), carboxyl groups on the CS and CMC macromolecules dissociated in aqueous media and converted to negatively charged carboxylate ions, leading to higher electrostatic repulsion and thus, water penetrating into the hydrogel matrix (Barkhordari and Yadollahi, 2016; Barkhordari *et al.*, 2014).

The effect of the content of ZnO nanoparticles on swelling degree of bionanocomposite hydrogel beads was also investigated. The swelling capacity was enhanced as the amount of ZnO NPs in the hydrogel increases (Khorasani *et al.*, 2018). Hence, CMC/CS/ZnO samples can absorb excess water. CMC/CS/ZnO nanocomposite beads increased rapidly and reached a higher swelling ratio. However, CCZ7, CCZ8, and CCZ9 samples containing 10 % ZnO nanoparticles and samples with components number CCZ10, CCZ11, and CCZ12 containing 15% ZnO nanoparticles had more swelling compared to CCZ4, CCZ5, and CCZ6 samples containing 5% of ZnO nanoparticles. Thus, with increasing concentrations of ZnO nanoparticles, the swelling rate increased (Rakhshaei *et al.*, 2019; Gunasekaran *et al.*, 2006).

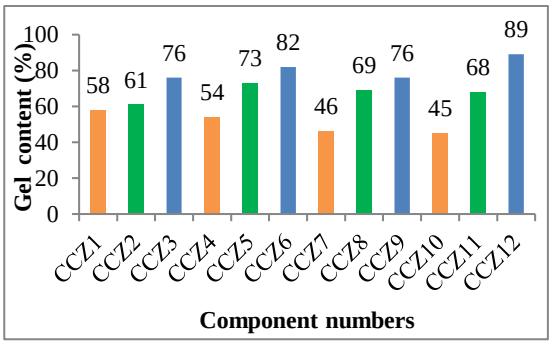

Figure 8. Gel content measurement of ZnO nanocomposite hydrogel beads in different component number

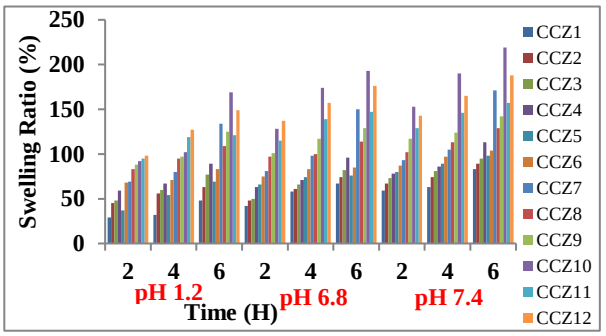

Figure 9. Swelling behavior of ZnO nanocomposite hydrogel beads at pH values of 1.2, 6.8 and 7.4 in different component number

3.10 Drug Loading

The effect of ZnO nanoparticles on DOX encapsulation was investigated via the prepared nanocomposite beads with the doxorubicin loading data obtained shown in Figure 8. It was clear from this figure that the content of doxorubicin as an anticancer drug loaded in the hydrogels increased enhancing the amount of ZnO NPs. The increase in the drug loading percentage is attributed to two reasons. Firstly, the existence of ZnO nanoparticles into the prepared nanocomposite beads created a high amount of pores and free spaces into these beads, and thus, more drug molecules penetrated within hydrogel beads. Meanwhile, there were hydrogen bonding and electrostatic attraction interactions between doxorubicin and ZnO nanoparticles. Secondly, these interactions resulted in the increase in the drug loading percentage of nanocomposite beads containing high amounts of ZnO nanoparticles. From the obtained results, it can be concluded that the encapsulation of doxorubicin by the prepared hydrogel beads rose upon adding ZnO nanoparticles (Gholamali *et al.*, 2019).

3.11 Drug Releasing

The behavior of drug release of DOX loaded CMC/CS/ZnO nanocomposite beads containing different amounts of ZnO nanoparticles at various pHs of 1.2, 6.8 and 7.4 was studied for 300 min. Also, the relationship between release of doxorubicin hydrogel beads versus time was examined with the weight ratios of CMC/CS (3:1, 1:1, and 1:3) with various concentrations of ZnO-NPS as shown in Figures 10 to 13. As seen in figures 10 to 13, the highest amount of drug release in hydrogels at 300 min in phosphate buffers at pH 6.8 and 7.4 was compared to acidic medium (pH 1.2). The drug release of doxorubicin from DOX loaded onto neat CMC/CS and CMC/CS/ZnO nanocomposites in acidic medium, pH 6.8 and 7.4 phosphate buffers revealed different release mechanisms which depended on the type of cationic ions in the release medium. A possible explanation for this may be that in acidic medium, hydrogen bonds in CMC/CS hydrogels caused creation of hydrophobic networks a collapsed state. In addition, the carboxyl groups of CMC and CS are not ionized in the acidic medium. These factors can lead to the formation of insoluble CMC/CS beads for reserved drug release; hence, doxorubicin release from the hydrogels can be described by a controlled matrix diffusion mechanism. Nevertheless, at pH 6.8 and 7.4 of phosphate buffer, the carboxylic acid groups in the CMC and CS became ionized on the CMC chains causing elevated osmotic pressure and increased electrostatic repulsion between charged groups. Thus, the maximum swelling was observed at pH 7.4 phosphate buffer for CMC/CS hydrogel beads. As indicated in Figures 10 to 13, the release rate of DOX loaded on the hydrogel beads decreased with increases in the amount of ZnO nanoparticles, which plays a key role in prolonging drug release time of the ZnO nanoparticles in the nanocomposite hydrogel beads. There are two main reasons for the prolonged drug release of nanocomposite hydrogels, the presence of ZnO nanoparticles in the prepared hydrogel beads causes development of a long path for doxorubicin migration from the nanocomposite hydrogel beads in the release medium compared to the pure CMC/CS beads, resulting in prolonged release time. In addition, electrostatic adsorption interactions and the hydrogen bonding between ZnO nanoparticles in nanocomposite hydrogel beads and doxorubicin could reduce the initial release of DOX from the prepared beads (Gholamali, 2019; Zare-Akbari *et al.*, 2019).

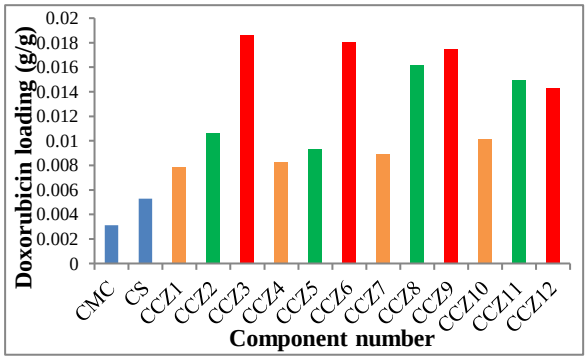

Figure 10. The amount of doxorubicin loaded into CS, CMC, and different component number

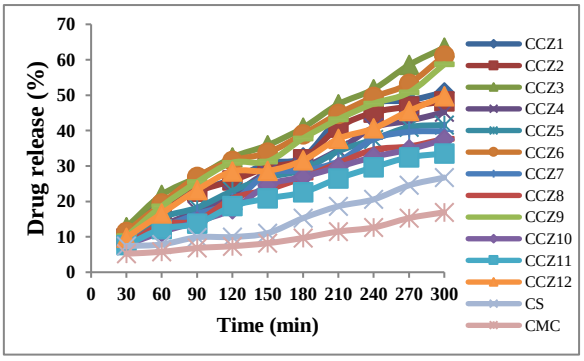

Figure 11. The percentage of drug released from CS, CMC, and different component number at pH value of 1.2

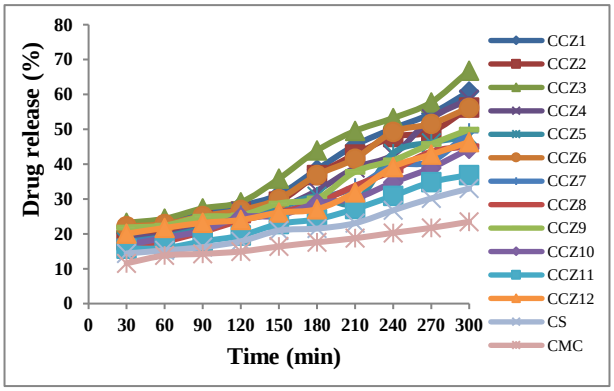

Figure 12. The percentage of drug released from CS, CMC, and different component number at pH value of 6.8

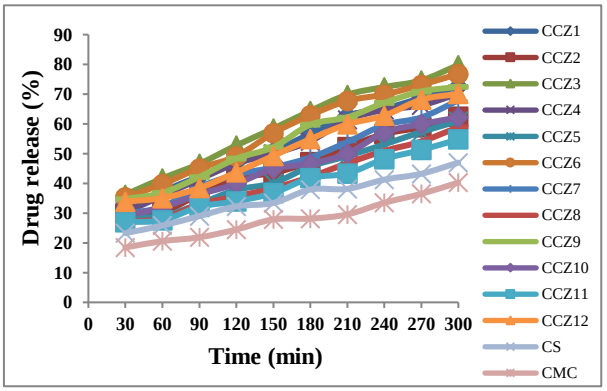

Figure 13. The percentage of drug released from CS, CMC, and different component number at pH value of 7.4

4. Conclusion

In the present work, the nanocomposite hydrogel beads were successfully synthesized by dispersing ZnO nanoparticles into CMC/Chitosan matrix. Asparagus stalk end was used as a raw material to produce carboxymethyl cellulose (CMC). The alkali solution is the main parameter that affected all characteristics of CMC synthesized with various NaOH concentrations. The structural details of the hydrogel beads were characterized by XRD, TGDTA, SEM, FTIR, and UV-Vis techniques. According to XRD data, the nanocomposite bead confirmed the presence of ZnO NPs as the main crystalline phase in the CMC/Chitosan hydrogel network. FT IR spectroscopy revealed the interaction between CMC/Chitosan and ZnO indicated that the peaks related to ZnO had appropriate beading. SEM images showed good dispersion of ZnO on the surface of the beads. TGDTA data suggest that in addition to increasing the thermal stability of the samples and the residual content, the thermal degradation in the samples containing ZnO NPs is greater than in the samples without the nanoparticles. All spectra of the nanocomposite hydrogel beads showed a broad absorption band within the UV range of 200–400 nm because of the surface plasmon resonance effect. The intensity of the plasmon band grows with increasing the zinc sulphate concentration in the hydrogel beads and reaches higher wave numbers. It can be a result of an increase in the size of ZnO-NPs. The swelling behavior of nanocomposite beads was studied at pHs 1.2, 6.8 and 7.4. The results indicated that the swelling ratio of CMC/Chitosan/ZnO nanocomposite beads was significantly enhanced compared to pure beads, which depended on the concentration of ZnO NPs. The effect of ZnO NPs on drug release behavior was also studied. Doxorubicin was selected as an anticancer drug with the loading and release capacity of the drug in different nanocomposite beads. The loading and release behavior of doxorubicin in hydrogels showed that nanocomposite hydrogel beads loaded in the drug better than the pure chitosan beads, but the drug release from neat beads was higher than that of nanocomposite hydrogel beads. Based on these findings, it can be concluded that CMC/Chitosan/ZnO nanocomposite beads can be introduced as a new bio-compatible carrier for controlled delivery of anticancer drugs such as doxorubicin.

Acknowledgment

The authors gratefully acknowledged the receipt of research funding for this research from the Asia Research Centre, University of Yangon. We would like to express my special thanks Dr Tin Maung Tun, Rector, University of Yangon who gave us the opportunity to do this research.

References

Abdelghany, A. M., A. A. Menazea and A. M. Ismail. (2019). "Synthesis,Characterization and Antimicrobial Activity of Chitosan/Polyvinyl Alcohol Blend Doped with *Hibiscus Sabdariffa L.* Extract", *Journal of Molecular Structure.*, **1197**, 603-609

Affes, S., A. Inmaculada, A. Niuris, H. Angeles, N. Moncef and M. Hana. (2021). "Chitosan Derivatives-Based Films as pH-Sensitive Drug Delivery Systems with Enhanced Antioxidant and Antibacterial Properties", *International Journal of Biological Macromolecules.*, **182**, 730-742

Aung Than Htwe, Hnin Wutt Yee Htun, Yamin Thet, May Thazin Kyaw, Ngwe Sin, Win Pa Pa Phyo and Cho Cho. (2022). "Preparation and Chaacterization of Carboxymethyl Cellulose Derived from Asparagus Stalk End ", *JARC-UY.*, **8**(1&2), 114-127

Azady, A. R., S. Ahmed and S. Islam. (2021). "A Review on Polymer Nanocomposite Hydrogel Preparation, Characterization, and Applications", *European Journal of Chemistry*, **12**(3), 329-339

Bajpai, S. K., N. Chand and V. Chaurasia. (2010). "Investigation of Water Vapor Permeability and Antimicrobial Property of Zinc Oxide nanoparticles-Loaded Chitosan-Based Edible Film", *J. Appl. Polym. Sci.*, **115**, 674-683

Barkhordari, S. and M. Yadollahi. (2016). "Carboxymethyl Cellulose Capsulated Layered Double Hydroxides/Drug nanohybrids for Cephalexin Oral Delivery", *Appl. Clay Sci.*, **121-122**, 77-85

Barkhordari, S., M. Yadollahi and H. Namazi. (2014). "pH Sensitive Nanocomposite Hydrogel Beads Based on Carboxymethyl Cellulose/Layered Double Hydroxide as Drug Delivery Systems", *J. Polym. Res.*, **21**(6), 1-9

Bhuyan, T., K. Mishra, M. Khanuja, R. Prasad and A. Varma. (2015). "Biosynthesis of Zinc Oxide Nanoparticles from Azadirachta Indica for Antibacterial and Photocatalytic Applications", *Mater Sci Semicond Process.*, **32**, 55-61

Cai, Y., H. Lihua, T. Xia, S. Jiaqi, C. Bifen, Z. Feibai, Z. Mouming, Z. Qiangzhong and P. V. Meeren. (2021). "Effect of pH on Okara Protein- carboxymethyl Cellulose Interactions in Aqueous Solution and at Oil-Water Interface", *Food Hydrocolloids*, **113**, 1-14

Catton, E. B., M. L. Ross and P. Asuri. (2021). "Multifunctional Hydrogel Nanocomposites for Biomedical Applications", *Polymers* , **13**(856), 1-14

Gaharwar, A. K., N. A. Peppas and A. Khademhosseini. (2014). "Nanocomposite Hydrogels for Biomedical Applications", *Biotechnol. Bioeng.*, **111**(3), 441-453

Gholamali, I. (2019). "Stimuli-Responsive Polysaccharide Hydrogels for Biomedical Applications: a Review", *Regen. Eng. Transl. Med.*, 1-24

Gholamali, I. and M. Yadollahi. (2020). "Doxorubicin-Loaded Carboxymethyl Cellulose/Starch/ZnO Nanocomposite Hydrogel Beads as an Anticancer Drug Carrier Agent", *International Journal of Biological Macromolecules* , **160**, 724-735

Gholamali, I., M. Asnaashariisfahani and E. Alipour. (2019). "Silver Nanoparticles Incorporated in pH-Sensitive Nanocomposite Hydrogels Based on Carboxymethyl Chitosan- Polyvinyl Alcohol for Use in a Drug Delivery System", *Regen. Eng. Transl. Med.*, 1-16

Gholamali, I., S. N. Hosseini, E. Alipour and M. Yadollahi. (2019). "Preparation and Characterization of Oxidized Starch/CuO Nanocomposite Hydrogels Applicable in a Drug Delivery System", *Polymers*, **71**(3-4), 1800118

Gunasekaran, S., T. Wang and C. Chai. (2006). "Swelling of pH-Sensitive Chitosan-Polyvinyl Alcohol Hydrogels", *J. Appl. Polym. Sci.*, **102**, 4665-4671

Iqbal, O., S. Shahid, A. Ghulam, R. Akhtar, H. Muhammad, A. Mehran and A. Zunaira. (2021). "Moxifloxacin Loaded Nanoparticles of Disulfide Bridged Thiolated Chitosan-Eudragit RS100 for Controlled Drug Delivery", *International Journal of Biological Macromolecules*, **182**, 730-742

Khorasani, M. T., A. Joorabloo, A. Moghaddam, H. Shamsi and Z. M. Moghadam. (2018). "Incorporation of ZnO Nanoparticles into Heparinised Polyvinyl Alcohol/Chitosan Hydrogels for Wound Dressing Application ", *Int. J. Biol. Macromol.*, **114**, 1203-1215

Klunklin, W., K. Jantanasakulwong, Y. Phimolsiripol, N. Leksawasdi, P. Seesuriyachan, T. Chaiyaso, C. Insomphun, S. Phongthai, P. Jantrawut, S. R. Sommano, W. Punyodom, A. Reungsang, T. M. P. Ngo and P. Rachtanapun. (2021). "Synthesis, Characterization, and Application of Carboxymethyl Cellulose from Asparagus Stalk End", *Polymers*, **13**(81), 1-15

Li, X. H., Y. G. Xing, W. L. Li, Y. H. Jiang and Y. L. Ding. (2010). "Antibacterial and Physical Properties of Polyvinyl Chloride- Based Film Coated with ZnO Nanoparticles", *Food Sci. Technol. Int.*, **16**(3), 225-232

Lotfy, V. F. and A. H. Basta. (2020). "Optimizing the Chitosan-Cellulose Based Drug Delivery System for Controlling the Ciprofloxacin Release Versus Organic/Inorganic Crosslinker, Characterization and Kinetic Study", *International Journal of Biological Macromolecules*, **165**, 1496-1506

Metwally, M. M., R. M. I. Youssef, S. Barkhordari, D. S. Badawy and M. Y. Abdelaal. (2022). "Synthesis of 3-Dimensional Chitosan/Carboxymethyl Cellulose/ZnO Biopolymer Hybrids by Ionotropic Geation for Application in Drug Delivery", *Egyt. J. Chem.*, **65(1)**, 299-307

Nagpal, K., S. K. Singh and D. N. Mishra. (2010). "Chitosan Nanoparticles: A Promising System in Novel Drug Delivery", *Chemical and Pharmaceutical Bulletin.*, **58**(11), 1423-1430

Niknia, N. and R. Kadkhodaee. (2017). "Factors Affecting Microstructure, Physicochemical and Textural Properties of a Novel Gum Tragacanth-PVA Blend Cryogel ", *Carbohydr. Polym.*, **115**, 475-482

Noshirvani, N., B. Ghanbarzadeh, R. R. Mokarram, M. Hashemi and V. Coma. (2017). "Preparation and Characterization of Active Emulsified Films Based on Chitosan-Carboxymethyl cellulose Containing Zinc Oxide Nanoparticles", *Int. J. boil. Macromol.*, **99**, 530-538

Pooresmaeil, M. and H. Namazi. (2018). "Preparation and Characterization of Polyvinyl Alcohol/β-cyclodextrin/GO-Ag Nanocomposite with Improved Antibacterial and Strength properties", *Polym. Adv. Technol.*, **30**, 447-456

Rachtanapun, P., and N. Rattanapanone. (2011). "Synthesis and Characterization of Carboxymethyl Cellulose Powder and Films from Mimosa Pigra Peel", *J. Appl. Polym. Sci.*, **122**, 3218-3226

Rakhshaei, R., H. Namazi, H. Hamishehkar, H. S. Kafil and R. Salehi. (2019). "In Situ Synthesized Chitosan-Gelatin/ZnO Nanocomposite Scaffold with Drug Delivery Properties: Higher Antibacterial and Lower Cytotoxicity Effects", *J. Appl. Polym. Sci.*, **136**, 47590

Rhim, W. J., S. I. Hong, H. M. Park and P. K. W. Ng. (2006). "Preparation and Characterization of Chitosan-Based nanocomposite Films with Antimicrobial Activity", *J. Agri. Food Chem.*, **54**, 5814-5822

Rodsamran, P. and R. Sothornvit. (2017). "Rice Stubble as a New Biopolymer Source to Produce Carboxymethyl Cellulose-Blended Films", *Carbohydr. Polym.*, **171**, 94-101

Sadhukhan, P., M. Kundu, S. Chatterjee, N. Ghosh, P. Manna, J. Das and P. C. Sil. (2019). "Targeted Delivery of Quercetin via pH-Responsive Zinc Oxide Nanoparticles for Breast Cancer Therapy", *Materials Science and Engineering:C*, **100**, 129-140

Satarkar, N. S., D. Biswal and J. Z. Hilt. (2010). "Hydrogel Nanocomposites: A Review of Applications as Remote Controlled Biomaterials", *Soft Matter.*, **6**(11), 2364-2371

Singh, T. A., J. Das and P. C. Sil. (2020). "Zinc Oxide Nanoparticles: A Comprehensive Review on Its Synthesis, Anticancer and Drug Delivery Applications as well as Health Risks", *Advances in Colloid and Interface Science*, 102317

Sun, X., C. Liu, A. M. Omer, W. Lu, S. Zhang, X. Jiang, H. Wu, D. Yu and X. K. Ouyang. (2019). "pH-Sensitive ZnO/Carboxymethyl Cellulose/Chitosan Bionanocomposite Bead for Colon-Specific Release of 5-Fluorouracil", *Int. J. Biol. Macromol.*, **128**, 468-479

Upadhyaya, L., J. Singh, V. Agarwal, A. C. Pandey, S. P. Verma, P. Das and R. P. Tewari. (2014). "Insitu Grafted Nanostructured ZnO/Carboxymethyl Cellulose Nanocomposites for Efficient Delivery of Curcumin to Cancer", *J. Polym. Res.*, **21(9)**, 1-9

Wang, F., Q. Zhang, K. Huang, J. Li, K. Wang, K. Zhang and X. Tang. (2020). "Preparation and Characterization of Carboxymethyl Cellulose Containing Quaternized Chitosan for Potential Drug Carrier", *International Journal of Biological Macromolecules*, **154**, 1392-1399

Yadollahi, M., H. Namazi and S. Barkhordari. (2014). "Preparation and Properties of Carboxymethyl Cellulose/ Layered Double Hydroxide Bionanocomposite Films ", *Carbohydr. Polym.*, **108**, 83-90

Yadollahi, M., I. Gholamali, H. Namazi and M. Aghazadeh. (2015). "Synthesis and Characterization of Antibacterial Carboxymethyl Cellulose/ZnO Nanocomposite Hydrogels", *Int. J. Biol. Macromol.*, **74**, 136-141

Yadollahi, M., S. S. Farhoudian, S. Barkhordari, I. Gholamali, H. Farhadnejad and H. Motasadizadeh. (2016). "Facile Synthesis of Chitosan/ZnO Bio-nanocomposite Hydrogel Beads as Drug Delivery Systems", *International Journal of Biological Macromolecules*, **82**, 273-278

Youssef, A. M., S. M. El-Sayed, H. H. Salama and A. Dufresne. (2016). "Enhancement of Egyptian Soft White Cheese Shelf Life Using a Novel Chitosan/Carboxymethyl Cellulose/Zinc Oxide Bionanocomposite Film", *Carbohydr. Polym.*, **151**(20), 9-19

Zare-Akbari, Z., H. Farhadnejad, B. Furughi- Nia, S. Abedin, M. Yadollahi and M. Khorsand-Ghayeni. (2019). "pH-Sensitive Bionanocomposite Hydrogel Beads Based on Carboxymethyl Cellulose/ZnO Nanoparticle as Drug Carrier", *Int. J. Biol. Macromol.*, **93**, 1317-1327

Zarrinkhameh, E., A. Zendehnam and S. M. Hosseini. (2015). "Fabrication of Polyvinyl Chloride Based Nanocomposite Thin Film Filled with Zinc Oxide Nanoparticles: Morphological, Thermal and Optical Characteristics ", *J. Ind. Eng. Chem.*, **30**, 295-301